

Multi-Classifier selection-fusion framework: application to NDT of complex metallic parts

Vahid Yaghoubi^{1,2}, Liangliang Cheng^{1,2}, Wim Van Paepengem¹, Mathias Kersemans¹

¹Mechanics of Materials and Structures (MMS), Ghent University, Technologiepark 46, B-9052 Zwijnaarde, Belgium.

²SIM M3 program, Technologiepark 48 , B-9052 Zwijnaarde, Belgium.

Abstract

Recent advances in computational methods, material science, and manufacturing technologies reveal promising potentials for using geometrically complex parts to optimize the performance of structural systems. However, this potential has not yet been activated partly due to the immaturity of nondestructive testing (NDT) of such complex parts. Process compensated resonance testing (PCRT) is one of the methods that are in the focus of researchers for this purpose. The key to success for the PCRT approach is to use high-frequency vibration data in conjunction with statistical pattern recognition methods for supervised classification of parts in terms of their structural quality. In this paper, a multi classifier selection-fusion framework based on the Dempster-Shafer theory is proposed. Two new weighting approaches are introduced to enhance the fusion performance, and as such the classification performance. The effectiveness of the proposed framework is validated by its application to six UCI machine learning datasets and one experimental dataset collected from polycrystalline Nickel alloy first-stage turbine blades with a variety of damage features. Comparison with four state-of-the-art fusion techniques shows the good performance of the introduced classifier selection-fusion framework.

Keywords: Classifier selection; Classifier fusion; Process compensated resonance testing; Nondestructive testing; Dempster-Shafer theory of evidence.

1 Introduction

The advanced computational methods, novel materials, and flexible manufacturing tools (e.g. additive manufacturing) provide a foundation to optimize the performance of complex systems by moving toward parts with complex geometries. However, nondestructive test and evaluation (NDT&E) of such components are not mature enough and thus, hinders their ever-increasing applications. An extensive review of the application of different NDT&E methods on parts with different levels of geometrical complexities has been conducted in [1]. It is concluded that for geometrically complex parts, only two NDE methods have the potential to identify defected samples: PCRT and X-ray μ CT. Albeit the advantages of employing X-ray μ CT [2], [3], it suffers from its slow procedure, expensive equipment, high level of required expertise to conduct the test, contrast problems for thick parts, and so on. Instead, the PCRT is more compatible with the new trend between the scientists and engineers to employ (statistical) learning algorithms in NDT&E due to its faster and more reliable online procedure with less operator training time and cost [4]–[12].

Process compensated resonance testing (PCRT), is an NDT&E and material characterization method that is based jointly on vibration data and statistical pattern recognition [13], [14]. In this approach, the resonant frequencies of several samples are first estimated. Then, depending on the shifts in those frequencies and by using a Mahalanobis-Taguchi system (MTS), the samples are classified into healthy and defected parts [15]. In PCRT, the frequency shift that may occur due to allowable process variations has been compensated, resulting in less number of samples with the wrong classification. The method has been successfully applied to several metallic and non-metallic cases [16], [17]. Recently, the current authors have proposed a classification framework for PCRT which is based on multi-dimensional Mahalanobis space coupled to binary particle swarm optimization for optimal feature ranking, and for more robust threshold determination between good/bad parts [18].

Several machine learning algorithms have been developed to reach the highest possible classification accuracy, e.g. discriminant analyses, decision tree, neural network, support vector machines, support vector data descriptors, etc. [19]. However, it is well-known that none of the classifiers can show high accuracies in all the applications and datasets due to the presence of different level of noise, outliers, nonlinearities, and data redundancy [20]. To deal with this problem, researchers suggested employing an ensemble of classification models to compensate for the weaknesses and to boost the strengths of each classifier [21][22], [23]. This, however, leads to two important questions: i) how to select classifiers from the pool of classifiers to keep the information and impose the diversity, and ii) how to combine their outputs to make a final decision.

One can impose diversity in the ensembles by using different classification methods, different numbers and types of features, different training samples, etc. [24]. To combine the classifiers, several methods have been proposed in the literature. From basic elementary operations like sum, average, maximum, and minimum of the outputs [21] to more advanced forms like majority voting [25], multilayered perceptrons [26], Bayes combination [27], fuzzy integrals [28], and Dempster-Shafer theory of evidence (DST) [29]. The last one is of interest in this paper due to its proven advantages over other combination methods [20], [24], [30]. For instance, Rothe et. al. conducted an extensive investigation to analyze the performance of all the fusion methods except for the Dempster-Shafer method [20]. It is concluded that in most cases, although the fusion methods cannot outperform the best individual classifier, they decrease the sensitivity to the outliers. In contrast, in [24], [30] it is shown that the Dempster-Shafer method could outperform the best individual classifier provided that the individual classifiers are independent. On the other hand, the problem of the DST method occurs when conflicting evidences come from different classifiers. In such cases, the fused output could lead to counter-intuitive results. Several researchers thus targeted to solve this problem by mainly two approaches: (i) by applying different preprocessing on the evidences to reduce their possible conflict, and (ii) modifying the combination rule. The former attracts more attention among researchers and is the focus of the current paper.

Deng et. al. [31] proposed to improve the basic probability assignment (BPA) based on the information extracted from the confusion matrix. In [32] the conflict between the evidences was reduced by employing Shannon's information entropy together with Fuzzy preference relations (FPR). Xiao [33] used the distance between the evidences to evaluate the support degree (SD) of the evidences. Then belief entropy and FPR were employed to adjust the SD. The adjusted SD is used as the weight for evidences prior to applying Dempster's rule of combination. In [34], a similarity between the BPAs was evaluated, and then by using it together with the belief entropy, the evidences were weighted before applying Dempster's rule of combination. In [35], a novel method has been developed to evaluate the BPAs based on the k-nearest neighbor algorithm. Wang et al. proposed to employ both subjective and objective weight for the evidences before combination [36]. Objective weight assesses the credibility of the evidences whereas, subjective weight evaluates the support degree of the evidences with respect to the focal element with the largest mass values.

Having the two aforementioned questions in mind, the major goal of the current paper is to develop a multi-classifier selection-fusion framework. To achieve this, first, a pool of classifiers is generated by using the common machine learning approaches. Then, it is proposed to select proper classifiers by maximizing the determinant of the information matrix generated by the classifiers' responses. In the

end, the proposed DST-based fusion method is applied to the selected classifiers. Besides, two new weighting factors are introduced and their effect on improving the performance of the fusion method is exploited.

The paper is organized as follows. In Section 2 some required background, including the PCRT method and the Dempster-Shafer theory are explained. In Section 3 different steps of the proposed algorithm are elaborated. In Section 4 the proposed framework is first applied to several UCI machine learning datasets and then it is applied to experimental test data collected from first-stage turbine blades with complex geometry and various damage features. In Section 5 concluding remarks are presented.

2 Background

In this section, some pertinent background will be given.

2.1 PCRT

PCRT is an NDT&E and material characterization method. In this method, by using one actuator and two sensors the frequency response function (FRF) of a test specimen is first measured. Then, important features such as resonant frequencies and associated Q-factors are estimated. This procedure is performed for several healthy and defected samples in order to create a database of vibrational features. In the end, the database is used to train a learning algorithm in order to separate the healthy and defected components [18].

2.2 Dempster-Shafer theory of evidence

Dempster-Shafer theory (DST) of evidence [29], is an important method for presenting uncertain knowledge. It provides a foundation to fuse the uncertain information obtained from different sources to have more concrete statistical inferences. DST is defined as follows.

Let $\theta_1, \theta_2, \dots, \theta_K$ be a finite number of possible hypotheses describing a phenomenon. A set with all these hypotheses is called *Frame of discernment*, i.e. $\Theta = \{\theta_1, \theta_2, \dots, \theta_K\}$. Its powerset denoted by 2^Θ is a set of all its subsets including the null set \varnothing and itself Θ .

Basic probability assignment (BPA), $m(\cdot)$, is a function that assigns a value in the bounded range $[0, 1]$ to every subset \mathcal{A} of Θ with the following conditions,

$$\begin{cases} m(\varphi) = 0 \\ \sum_{\mathcal{A} \in 2^\Theta} m(\mathcal{A}) = 1 \end{cases} \quad (1)$$

In contrast to probability theory in which a value is assigned to each individual hypotheses θ_i , in belief theory, one can assign a value to a composite hypothesis \mathcal{A} , i.e. $\mathcal{A} = \{\theta_1, \theta_2\}$, without any overcommitment to either. This means some “ignorance” is associated with \mathcal{A} that could lead to $m(\mathcal{A}) + m(\bar{\mathcal{A}}) \leq 1$ with $\bar{\mathcal{A}}$ as the complement of \mathcal{A} .

Combination rule provides a methodology to combine different BPAs in the frame of discernment Θ . It is defined as

$$m(\mathcal{A}) = (m_1 \oplus m_2)(\mathcal{A}) = \begin{cases} \frac{m_{12}(\mathcal{A})}{1 - m_{12}(\varphi)} & \mathcal{A} \subset \Theta, \mathcal{A} \neq \varphi \\ 0 & \mathcal{A} = \varphi \end{cases} \quad (2)$$

in which \oplus is the orthogonal sum,

$$m_{12}(\mathcal{A}) = \sum_{\mathcal{C}_1 \cap \mathcal{C}_2 = \mathcal{A}} m_1(\mathcal{C}_1)m_2(\mathcal{C}_2) \quad (3)$$

indicates the conjunctive consensus on \mathcal{A} among the sources \mathcal{C}_1 and \mathcal{C}_2 . Besides, the denominator is the normalization factor with,

$$m_{12}(\varphi) = \sum_{\mathcal{C}_1 \cap \mathcal{C}_2 = \varphi} m_1(\mathcal{C}_1)m_2(\mathcal{C}_2), \quad (4)$$

This can be extended when we have several BPAs as,

$$m(\mathcal{A}) = \left(((m_1 \oplus m_2) \oplus m_3) \dots \oplus m_n \right) (\mathcal{A}) \quad (5)$$

The combination rules (2) and (5) provide the required foundation for classifier fusion as explained in Section 3.3.

3 NDT methodology

Figure 1 shows the building block of an NDT procedure that is based on classifier fusion. Although the first two stages are crucial steps for any NDT approach, the main focus of this paper is in the last three stages. They are:

III) Classification: a pool of classifiers is the outcome of this step. This is explained in Section 3.1.

- IV) Classifier selection: in this step, some proper classifiers are selected for combination. This is elaborated in Section 3.2.
- V) Classifier fusion: in this step, the classifiers are combined to create a fused classifier with higher accuracy than those of each individual classifier. This is extensively discussed in Section 3.3.

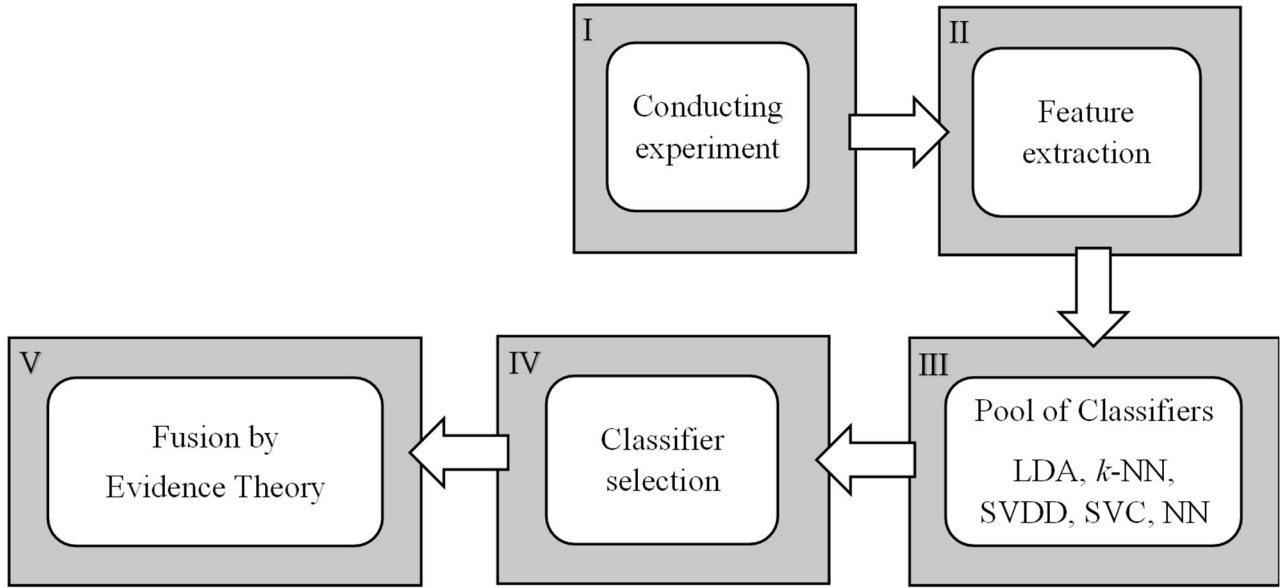


Figure 1. Flowchart of the NDT procedure.

3.1 Pool of classifiers

In this section, several classifiers that will be used to generate the pool of classifiers are explained. All the classifiers are implemented using the deep learning toolbox in Matlab 2019a.

3.1.1 Classifier generation

To generate a pool of classifiers, it is important to select classifiers that can deliver complementary information. For this purpose, three categories of classifiers with respect to their approach in combining the features before conducting classification have been selected.

- (i) The methods that linearly combined the features, e.g. Linear discriminant analysis (LDA) and k -nearest neighbor¹ (k -NN).
- (ii) The methods that combine the features by using some specific nonlinear function, e.g. support vector machine (SVM) and support vector data description (SVDD).

¹ k -NN uses the features as they are without any combination with the other features. this can be seen as a specific type of linear combination of features.

- (iii) The methods that combine the features by using any type of nonlinear functions, e.g. Neural Network (NN).

In the following, the methods mentioned above are briefly explained. For this purpose, let $\mathbf{X} \in \mathbb{R}^{n_s \times n_f}$ and $\mathbf{Y} \in \mathbb{Z}^{n_s \times n_c}$ be the matrices of input and output respectively. Here, n_s , n_f and n_c are the number of samples, features, and outputs/classes. Further, let $\widehat{\mathbf{Y}}_i \in \mathbb{R}^{n_s \times n_c}$ be the output of the classifier C_i , $i = 1, 2, \dots, N_c$.

linear discriminant analysis

In LDA, a normal distribution is first assumed for each class c_i , i.e. $P(X|c_i) = \mathcal{N}(\mu_i, \Sigma_i)$ for $i = 1, 2, \dots, n_c$, in which μ_i and Σ_i are mean and covariance matrix of the samples associated with class c_i . Then a projection Ψ of the features is pursued that maximize the between-class distances whilst minimize the within-class variance. For this purpose, let the within-class \mathbf{S}_w and between-class \mathbf{S}_b matrices be

$$\mathbf{S}_w = \sum_{i=1}^{n_c} P(c_i) \sum_{x \in c_i} (x - \mu_i)(x - \mu_i)^T \quad (6)$$

$$\mathbf{S}_b = \sum_{i=1}^{n_c} P(c_i) (\mu_i - \mu)(\mu_i - \mu)^T \quad (7)$$

where μ is the mean of all samples, $(\cdot)^T$ is the transpose operation, and $P(c_i) = \frac{n_i}{n_s}$ with n_i as the number of samples assigned to class c_i is the prior distribution of class c_i . Then the eigenvector of the matrix $\mathbf{S}_w^{-1} \mathbf{S}_b$ gives the projection matrix of our interest Ψ .

Then a new sample x_{new} belongs to the class with highest posterior probability defined as follows,

$$P(c_i | \Psi x_{\text{new}}) = P(c_i) P(\Psi x_{\text{new}} | c_i) \quad (8)$$

k-nearest neighbors

This approach requires no modeling. In k -NN, the new sample x_{new} is compared with its closes k training points and then its class estimated by using majority vote among the k neighbors. The distance could be measured in different metrics, here the linear correlation is selected. And k is selected to be an odd number in the range of [5, 15].

Support vector machines

In support vector machines (SVM) the features are first mapped through a nonlinear projection called *kernels*. By this, we could define nonlinear boundaries between classes. In this work, the kernel function is “Gaussian” with the parameters obtained through 10-fold cross-validation.

Support vector data description:

Support vector data description (SVDD) is an outlier detection or classification method that was inspired by SVM. Instead of separating the classes by a hyperplane, SVDD tries to obtain a spherically shaped boundary around the dataset. By employing *kernels*, one can obtain more flexible, yet closed boundaries.

In this approach, the center \mathcal{C} and radius \mathcal{R} of the sphere are obtained from the training samples and the new sample x_{new} is classified as normal, provided that

$$\|x_{new} - \mathcal{C}\| \leq \mathcal{R} \quad (9)$$

otherwise, it is an outlier. Here, $\|\cdot\|$ indicates any norm of the vector (\cdot) .

Neural network

Neural network (NN) with backpropagation is a learning method inspired by the human brain to learn gradually. In this approach first, the features are linearly combined and then, the boundaries are obtained as a nonlinear function of them. The complexity and strength of this nonlinearity depend on the activation functions, number of neurons, and layers. This leads to a very powerful learning method.

In this work, a NN model with one hidden layer and 10 neurons has been selected. All of them have the “tansig” activation function. The parameters are estimated by using the Levenberg-Marquardt optimization approach. To avoid overfitting, 10-fold cross-validation is used.

3.1.2 Performance evaluation

To evaluate the performance of the trained classifiers the so-called confusion matrix, see Figure 2, is implemented. Based on this matrix, several decisive measures have been developed that are presented in Table 1. The main measure here is accuracy (Acc) that indicates the portion of the samples that are correctly classified, Eq. (10). The other measures are sensitivity, Eq. (11), and specificity, Eq. (12), that can be considered respectively as the accuracy of the positive and negative classes.

$$Acc = \frac{TP + TN}{TP + FP + FN + TN} \quad (10)$$

$$Sns = \frac{TP}{TP + FN} \quad (11)$$

$$Spc = \frac{TN}{TN + FP} \quad (12)$$

		True condition	
		Good	Bad
Predicted condition	Good	True Positive (TP)	False Positive (FP)
	Bad	False Negative (FN)	True Negative (TN)

Figure 2. Confusion matrix

3.2 Classifier selection:

To select classifiers, two conditions should be met:

- (i) Optimizing the information content of the trained samples
- (ii) Imposing diversity in the trained classifiers

For this purpose, first, the matrix $\tilde{\mathbf{Y}}$ is obtained as follows,

$$\tilde{\mathbf{Y}} = [\text{vec}(\hat{\mathbf{Y}}_1), \text{vec}(\hat{\mathbf{Y}}_2), \dots, \text{vec}(\hat{\mathbf{Y}}_{N_c})] \in \mathbb{R}^{(n_s \times n_c) \times N_c} \quad (13)$$

in which $\text{vec}(\cdot)$ is the vectorized form of the matrix (\cdot) . Then, in analogy to the D-optimality [37], by selecting one column at a time, maximum determinant of information matrix, i.e. $|\tilde{\mathbf{Y}}^T \tilde{\mathbf{Y}}|$, is pursued.

To satisfy the second condition, the methods belonging to the last two categories i.e. SVC, SVDD, and NN, are imposed to the selected classifiers if they were not already selected. The procedure of classifier selection is presented in Algorithm 1.

Algorithm 1. Classifier selection algorithm

Input: $\tilde{\mathbf{Y}}, \tilde{\mathbf{Y}}_t = \emptyset, \mathbf{inf} = \emptyset$

while $\tilde{\mathbf{Y}} \neq \emptyset$ **do**

For $i = 1$ **to** number of columns in $\tilde{\mathbf{Y}}$ **do**

$\tilde{\mathbf{Y}}_t \leftarrow [\tilde{\mathbf{Y}}_t \tilde{\mathbf{Y}}(:, i)]$

$di(i) = \left| \tilde{\mathbf{Y}}_t^T \tilde{\mathbf{Y}}_t \right|$

$id = argmax(di)$

$\tilde{\mathbf{Y}}_t \leftarrow [\tilde{\mathbf{Y}}_t \tilde{\mathbf{Y}}(:, id)]$

$\mathbf{inf} \leftarrow [\mathbf{inf}, di(id)]$

 Remove $\tilde{\mathbf{Y}}(:, id)$

$mi = argmax(\mathbf{inf})$

$\tilde{\mathbf{Y}}_s := \tilde{\mathbf{Y}}_t(:, 1: mi)$

if $\text{vec}(\hat{\mathbf{Y}}_{SVC}) \notin \tilde{\mathbf{Y}}_s$ **then**

$\tilde{\mathbf{Y}}_s \leftarrow [\tilde{\mathbf{Y}}_s \text{vec}(\hat{\mathbf{Y}}_{SVC})]$

if $\text{vec}(\hat{\mathbf{Y}}_{SVDD}) \notin \tilde{\mathbf{Y}}_s$ **then**

$\tilde{\mathbf{Y}}_s \leftarrow [\tilde{\mathbf{Y}}_s \text{vec}(\hat{\mathbf{Y}}_{SVDD})]$

if $\text{vec}(\hat{\mathbf{Y}}_{NN}) \notin \tilde{\mathbf{Y}}_s$ **then**

$\tilde{\mathbf{Y}}_s \leftarrow [\tilde{\mathbf{Y}}_s \text{vec}(\hat{\mathbf{Y}}_{NN})]$

Output: $\tilde{\mathbf{Y}}_s$

3.3 Classifier fusion by DST

In this section, the application of DST to the classifier fusion is explained. In the literature, several variations of the DST have been proposed for classifier fusion [24], [30], [38], [39]. In this regard, let $\Theta = \{\theta_1, \dots, \theta_k, \dots, \theta_K\}$ be the frame of discernment in which θ_k is the hypothesis that the sample x belongs to class k . For classifier $C_i, i = 1, 2, \dots, N_c$, the associated ignorance and the belief in θ_k are indicated respectively by $m_i(\Theta)$ and $m_i(\theta_k)$. Further, let $\mathbf{w}_i \in \mathbb{R}^{1 \times K}$ and $\mathbf{r}_i \in \mathbb{R}^{1 \times K}$ be its weighting factor and reference vector. The BBAs will be combined based on the combination rule in Eqs. (2) and (5) to produce the new output vector \mathbf{y} as follows,

$$\mathbf{y} = m(\theta_k) = m_1(\theta_k) \oplus \dots \oplus m_{n_c}(\theta_k) \quad (14)$$

Different methods have been proposed to estimate the BPAs [24], [38], [39]. In this paper, a distance-based method has been implemented. In this regard, let

$$\mathbf{D}_i = \phi(\mathbf{R}_i, \mathbf{w}_i \otimes \widehat{\mathbf{Y}}_i) = [\mathbf{d}_i^1, \dots, \mathbf{d}_i^k, \dots, \mathbf{d}_i^K] \in \mathbb{R}^{n_s \times K} \quad (15)$$

be a proximity measure between the reference matrix $\mathbf{R}_i = \mathbf{r}_i \otimes \mathbf{1} \in \mathbb{R}^{n_s \times K}$ and $\widehat{\mathbf{Y}}_i$. Here $\mathbf{1} \in \mathbb{R}^{n_s \times 1}$ is an all-one vector and \otimes is the Kronecker product. ϕ could be any function and/or norm that could represent this proximity. Here $\phi(\mathbf{R}_i, \mathbf{w}_i \widehat{\mathbf{Y}}_i) = \exp(-\|\mathbf{R}_i - \mathbf{w}_i \otimes \widehat{\mathbf{Y}}_i\|^2)$. Considering ε_i as the ignorance of \mathcal{C}_i , BPAs are defined as

$$m_i(\theta_k, \mathbf{R}_i, \varepsilon_i) = \frac{\mathbf{d}_i^k}{\sum_{k=1}^K \mathbf{d}_i^k + \varepsilon_i} \quad (16)$$

$$m_i(\Theta, \mathbf{R}_i, \varepsilon_i) = 1 - \sum_{k=1}^K m_i(\theta_k, \mathbf{R}_i, \varepsilon_i) = \frac{\varepsilon_i}{\sum_{k=1}^K \mathbf{d}_i^k + \varepsilon_i} \quad (17)$$

The last step is to obtain the reference vector \mathbf{R}_i and also the ignorance ε_i . Inspired by [30], the reference vector is obtained by minimizing the distance between the combined-model output $\mathbf{y}(\mathbf{R}_i, \varepsilon)$ defined in Eq. Error! Reference source not found. and the true output \mathbf{Y} , i.e.

$$\mathbf{R}_i, \varepsilon = \operatorname{argmin}(\|\mathbf{y}(\mathbf{R}_i, \varepsilon) - \mathbf{Y}\|) \quad (18)$$

Weighting factor \mathbf{w}

The last step is to define a weighting factor \mathbf{w}_i . Five different weightings based on the confusion matrix (see Figure 2) are presented in Table 1. The \mathbf{w}_0 corresponds to unweighted version of the fusion algorithm. Weighting $\mathbf{w}_1 - \mathbf{w}_4$ have been introduced in the literature [40][41][31], However, in this paper, they are used in a new fashion. The last weighting, i.e. \mathbf{w}_5 , is introduced here as the combination of overall accuracy and class accuracies by applying the Dempster rule of combination as follows,

$$\mathbf{w}_5 = [Acc\ Acc] \oplus [Sns\ Spc] \quad (19)$$

in which Acc , Sns , and Spc are defined in Eqs. (10)-(12).

Another scheme to boost the performance of the combination method is obtained by applying the Dempster rule of combination on the outputs of all weightings. That can be interpreted as the fusion of fusions, i.e.

$$\mathbf{y}_6 = \bigoplus_{i=0}^5 \mathbf{y}_i \quad (20)$$

The efficacy of these weightings in improving the performance of the proposed fusion technique will be investigated in the following sections.

Table 1. Weighting factors

Response	Weight	Formulation	Description	Reference
P_0	\mathbf{w}_0	$\mathbf{1}$	Unweighted form	---
P_1	\mathbf{w}_1	Acc_i	$Acc = \frac{TP + TN}{TP + FP + FN + TN}$	
P_2	\mathbf{w}_2	$[Sns_i Spc_i]$	$Sns = \frac{TP}{TP + FN}$ $Spc = \frac{TN}{TN + FP}$	[41]
P_3	\mathbf{w}_3	$[PPV_i NPV_i]$	$PPV = \frac{TP}{TP + FP}$ $NPV = \frac{TN}{TN + FN}$	[40]
P_4	\mathbf{w}_4	$\mathbf{w}_2 \oplus \mathbf{w}_3$	----	[31]
P_5	\mathbf{w}_5	$\mathbf{w}_1 \oplus \mathbf{w}_2$	----	----
P_6	\mathbf{w}_6	$\bigoplus_{i=0}^5 P_i$	----	----

3.4 Prediction

The overall procedure of the proposed multi-classifier selection-fusion framework is presented in Algorithm 2. To apply the method on a new sample, following steps should be taken:

- (i) Classify the sample by the selected individual classifiers C^s
- (ii) Evaluate the BPAs (m^s) by obtaining the proximity of the classifiers' responses and their associated references
- (iii) Combine the BPAs by the Dempster's rule

Algorithm 3 presents the procedure to predict the health status of a new sample.

Algorithm 2. The proposed classifier selection-fusion framework

Inputs: X : input matrix, Y : output matrix, C : classifier

for $i = 1$ to N_c **do**

 Train classifier C_i

 Evaluate $\hat{Y}_i = C_i(X)$

for $j = 1$ to 7 **do**

 Evaluate $\mathbf{w}_{i,j}$ s using Table 1

Generate $\tilde{Y} = [\text{vec}(\hat{Y}_1), \text{vec}(\hat{Y}_2), \dots, \text{vec}(\hat{Y}_{N_c})]$

Obtain \tilde{Y}_s and C^s using Algorithm 1

for $i = 1$ to *columns in* \tilde{Y}_s **do**

 Generate $\hat{Y}_i^s = \text{vec}^{-1}(\tilde{Y}_s(:, i))$

for $j = 1$ to 7 **do**

$D_{i,j} = \exp(-\|\mathbf{R}_{i,j} - \mathbf{w}_{i,j} \otimes \hat{Y}_i^s\|^2)$

$m_i(\theta_k, \mathbf{R}_{i,j}, \varepsilon_{i,j})$ by Eq. (16)

$m_i(\Theta, \mathbf{R}_{i,j}, \varepsilon_{i,j})$ by Eq. (17)

 Evaluate $\mathbf{y}(\mathbf{R}_j, \varepsilon_j)$ using Eqs. (12), (5), and (2)

$\mathbf{R}_j, \varepsilon_j = \text{argmin}(\|\mathbf{y}(\mathbf{R}_j, \varepsilon_j) - Y\|)$

Pool of classifiers

Classifier selection

Classifier fusion

Output: $\mathbf{R}, \varepsilon, \mathbf{w}$

Algorithm 3. Class prediction of the new sample \mathbf{x}_{new}

Input: $\mathbf{x}_{new}, \mathbf{R}, \varepsilon, \mathbf{w}$, trained classifiers C^s

For all selected classifiers C^s

 Evaluate $\hat{y}_i^s = C_i^s(\mathbf{x}_{new})$

for $j = 1$ to 7 **do**

$D_{i,j} = \exp(-\|\mathbf{R}_{i,j} - \mathbf{w}_{i,j} \otimes \hat{y}_i^s\|^2)$

$m_i(\theta_k, \mathbf{R}_{i,j}, \varepsilon_{i,j})$ by Eq. (16)

$m_i(\Theta, \mathbf{R}_{i,j}, \varepsilon_{i,j})$ by Eq. (17)

 Evaluate $\hat{y}(\mathbf{R}_j, \varepsilon_j)$ using Eqs. (12), (5), and (2)

Output: \hat{y}

4 Application

In this section, the proposed classifier selection-fusion framework was first applied to six UCI machine learning datasets [37]. It is then applied to an experimental dataset collected by the PCRT method from equiax Polycrystalline Nickel alloy first-stage turbine blades with complex geometry and various damage features. The method has been applied using the unweighted version as well as the six different weightings.

To highlight the performance of the fusion method in enhancing the classification accuracy, its outcome has been compared with 4 state-of-the-art DST-based fusion methods. These methods are abbreviated by M_1 [34], M_2 [42], M_3 [33], and M_4 [36].

4.1 UCI datasets

In this section, the method has been applied to six UCI machine learning datasets which have two classes. The detailed descriptions of these datasets are presented in Table 2. For each dataset, the classifiers are trained by the 10-fold cross-validation. The final outcome is the average over the 10 models' outputs. The accuracy of the models assessed on the test dataset is presented in Table 3. In each dataset, the most accurate models are bold and underlined. By applying the proposed classifier selection procedure on the models' outputs over the training dataset, proper classifiers have been chosen. They are shown by \square in the table.

To combine the classifiers, two scenarios are presented, (i) all trained classifiers are used for fusion. (ii) only the classifiers selected by the selection procedure are used for fusion. Their results are respectively presented in Table 4 and Table 5.

Each table has two sections: unweighted and weighted. In the unweighted parts, the unweighted form of the fusion method i.e. P_0 , is compared with four other methods. In the weighted part, the combination technique in conjunction with six different weightings is presented. In each section, the maximum achieved accuracy is shown in bold. The last column indicates the number of times that each method leads to the maximum accuracy, i.e. number of occurrence or Occ. in brief. For each dataset, the maximum accuracy obtained through fusion methods is underlined.

Table 2. general description of six UCI machine learning datasets [37]

	Number of samples (n_s)	Number of features (n_f)	Number of classes (n_c)	[Train Test] %
Diabetes	768	8	2	[50 50]
Breast Cancer	699	9	2	[50 50]
Glass	214	9	2	[50 50]
Ovarian Cancer	216	63	2	[50 50]
Crab	200	6	2	[50 50]
Ionosphere	351	33	2	[50 50]

Table 3. Accuracy (in percent) on the test set of UCI datasets for the different classification methods. For each dataset, the selected classifiers are shown by .

	Diabetes		B. Cancer		Glass		O. Cancer		Crab		Ionosphere	
	Acc.	Sel.	Acc.	Sel.	Acc.	Sel	Acc.	Sel.	Acc.	Sel.	Acc.	Sel.
LDA	76.56	<input checked="" type="checkbox"/>	97.71	<input checked="" type="checkbox"/>	93.51	<input checked="" type="checkbox"/>	55.96	<input checked="" type="checkbox"/>	92.00		87.50	<input checked="" type="checkbox"/>
5-NN	67.70		90.57		97.22		89.90		94.00	<input checked="" type="checkbox"/>	88.06	<input checked="" type="checkbox"/>
7-NN	67.70		88.85		94.44		89.90		94.00		86.93	
9-NN	69.27	<input checked="" type="checkbox"/>	88.57		93.51		89.90		92.00	<input checked="" type="checkbox"/>	86.93	<input checked="" type="checkbox"/>
11-NN	67.96		87.42		93.51		88.07		89.00		86.93	
13-NN	69.79		88.00		93.51		88.07		92.00		85.79	
15-NN	69.73		88.00	<input checked="" type="checkbox"/>	92.59	<input checked="" type="checkbox"/>	88.07	<input checked="" type="checkbox"/>	90.00	<input checked="" type="checkbox"/>	85.79	<input checked="" type="checkbox"/>
SVC	74.73	<input checked="" type="checkbox"/>	97.71	<input checked="" type="checkbox"/>	97.22	<input checked="" type="checkbox"/>	91.74	<input checked="" type="checkbox"/>	85.00	<input checked="" type="checkbox"/>	97.15	<input checked="" type="checkbox"/>
SVDD	76.04	<input checked="" type="checkbox"/>	94.00	<input checked="" type="checkbox"/>	92.59	<input checked="" type="checkbox"/>	83.48	<input checked="" type="checkbox"/>	90.00	<input checked="" type="checkbox"/>	83.52	<input checked="" type="checkbox"/>
NN	82.03	<input checked="" type="checkbox"/>	98.00	<input checked="" type="checkbox"/>	96.29	<input checked="" type="checkbox"/>	91.74	<input checked="" type="checkbox"/>	96.00	<input checked="" type="checkbox"/>	93.75	<input checked="" type="checkbox"/>

Table 4. Accuracy (in percent) on the test set of UCI datasets obtained by fusion of **all individual** classifiers.

		Diabetes	B. Cancer	Glass	O. Cancer	Crab	Ionosphere	Occ.
Unweighted	M_1	73.70	94.86	95.37	89.91	95.00	89.20	2
	M_2	71.61	90.58	94.44	89.91	93.00	88.64	0
	M_3	71.85	93.71	95.37	89.91	95.00	89.20	1
	M_4	73.18	93.15	95.37	89.91	93.00	89.20	0
	P_0	73.70	95.14	96.30	90.83	95.00	96.02	6
Weighted	P_1	77.34	96.86	95.37	92.66	99.00	98.86	2
	P_2	71.61	98.29	97.22	90.83	93.00	94.32	2
	P_3	78.13	96.86	97.22	85.32	95.00	93.75	1
	P_4	81.00	98.28	95.37	89.90	96.00	97.73	1
	P_5	77.60	97.71	96.30	87.15	98.00	93.75	0
	P_6	80.21	97.71	97.22	93.58	97.00	98.30	2

Table 5. Accuracy (in percent) on the test set of UCI datasets obtained by fusion of **selected** classifiers.

		Diabetes	B. Cancer	Glass	O. Cancer	Crab	Ionosphere	Occ.
Unweighted	M_1	79.68	96.86	96.29	91.74	95.00	91.47	0
	M_2	78.39	94.86	97.22	90.83	95.00	90.34	1
	M_3	77.39	98.00	96.29	91.74	95.00	90.91	1
	M_4	78.13	95.43	96.29	90.83	93.00	91.48	0
	P_0	80.99	97.71	96.29	92.66	97.00	97.15	4
Weighted	P_1	77.86	98.86	97.22	91.74	99.00	95.45	2
	P_2	70.83	98.29	95.37	94.49	96.00	98.30	1
	P_3	77.60	98.57	97.22	85.32	97.00	95.45	0
	P_4	74.74	98.00	97.22	80.81	94.00	96.02	0
	P_5	82.03	98.29	95.37	89.91	96.00	98.86	2
	P_6	77.08	98.57	98.15	94.49	97.00	97.15	2

Comparing the weighted part with the unweighted parts in table 4 and table5 reveals the added value of using weightings. However, the selection of the best weighting is very application dependant and it seems impossible to select one weighting which works best for all applications. Furthermore, by comparing Table 5 with Table 4, one can simply observe that the selection procedure can improve the accuracy of all fusion techniques. In the end, it can be concluded that the proposed classifier selection-fusion framework together with proper weightings could lead to the best classification accuracy. It could also outperform the most accurate single classifier. However, choosing proper weighing is not a trivial task. This will elaborate in the following section.

4.2 First-stage turbine blades

In this section, the proposed classification algorithm is applied to Equiax Polycrystalline Nickel alloy first-stage turbine blades that have complex geometries and various damage features. Two views of its CAD model are shown in Figure 3. The cooling channel in the middle can be seen in the transparent view. Vibrational data has been collected from each blade in the range of [3, 38] kHz, see Figure 4. From the FRFs, 16 frequencies, F_i $i = 1,2, \dots, 16$, and 16 quality factors, Q_i $i = 1,2, \dots, 16$, are extracted which will be used as features for the classifiers. To create a database 192 healthy and 33 defected blades have been measured. The damages in the blades range from microstructure changes due to over-temperature, airfoil cracking, inter-granular attack (corrosion), to thin walls due to casting, maintenance and repair operations, and/or service wear. It should be emphasized that prior to apply any classification methodology, the health condition of the samples has been determined by some means, e.g. X-ray, visual testing, penetrant testing, ultrasonics, operator experience, etc., and that knowledge is used to train and evaluate the performance of the proposed classification approach.

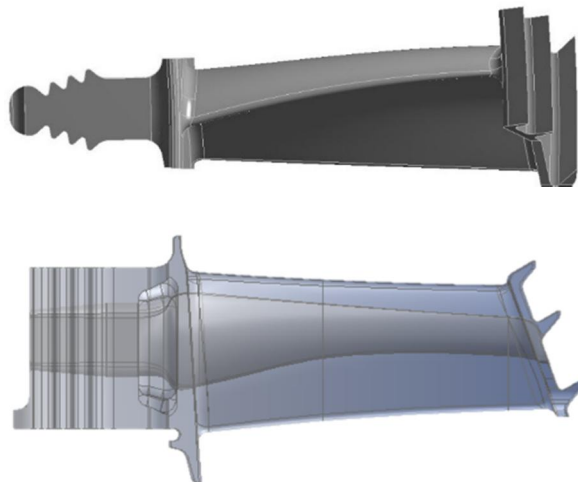


Figure 3. Two views of the CAD model of the Equiax Polycrystalline Nickel alloy first-stage turbine blade. Bottom plot shows a transparent view to highlight the internal cooling channel.

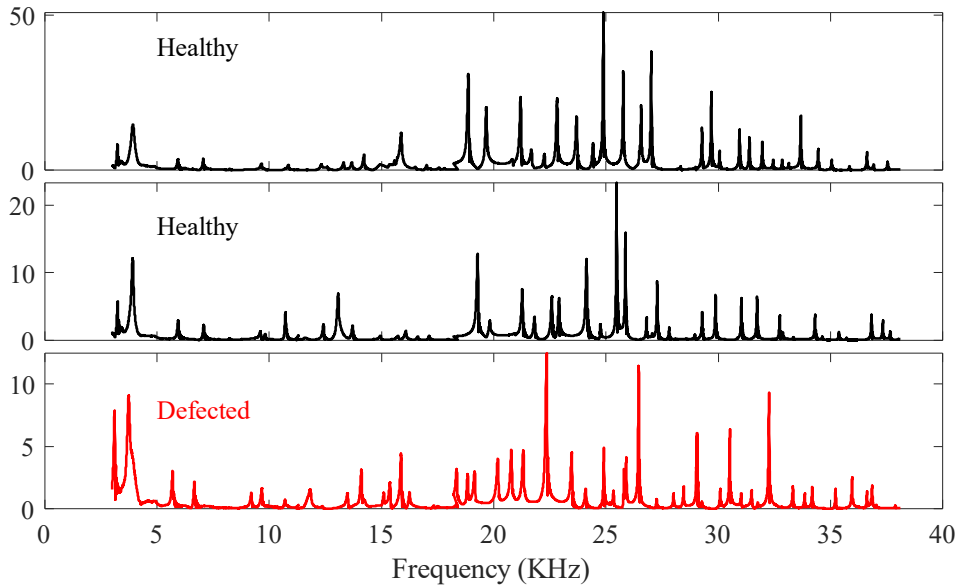


Figure 4. Three examples of FRFs. Two top FRFs have been collected from healthy blades and the bottom one was from a defected blade.

To commence the procedure, the data has to be randomly divided into two parts, 50% (113 samples) for training, and 50% (112 samples) for testing the classifiers. The accuracy of the trained classifiers are assessed on both the training and the test dataset, and is reported in Table 6. The models with the highest accuracy are bold and underlined. The proposed classifier selection methodology has been applied to the individual classifiers' outputs. Its outcome is shown in Figure 5. In order to extract the maximum information from the trained classifiers, only four classifiers should be chosen. However, to impose diversity in the classifiers, the SVC approach is also added to the selected classifiers (see also algorithm 1). One can see the selected classifiers in the last row of Table 6, shown by .

Table 6. Accuracy (in percent) of the trained classifiers assessed on training and test dataset. The most accurate models are bold and underlined. The classifiers selected for combination are shown by .

	LDA	5-NN	7-NN	9-NN	11-NN	13-NN	15-NN	SVC	SVDD	NN
Train	99.26	94.85	94.85	92.65	91.18	91.18	91.18	98.53	98.53	97.79
Test	92.22	92.22	92.22	91.11	91.11	91.11	90.00	95.56	<u>97.78</u>	<u>97.78</u>
Sel.	<input checked="" type="checkbox"/>						<input checked="" type="checkbox"/>	<input checked="" type="checkbox"/>	<input checked="" type="checkbox"/>	<input checked="" type="checkbox"/>

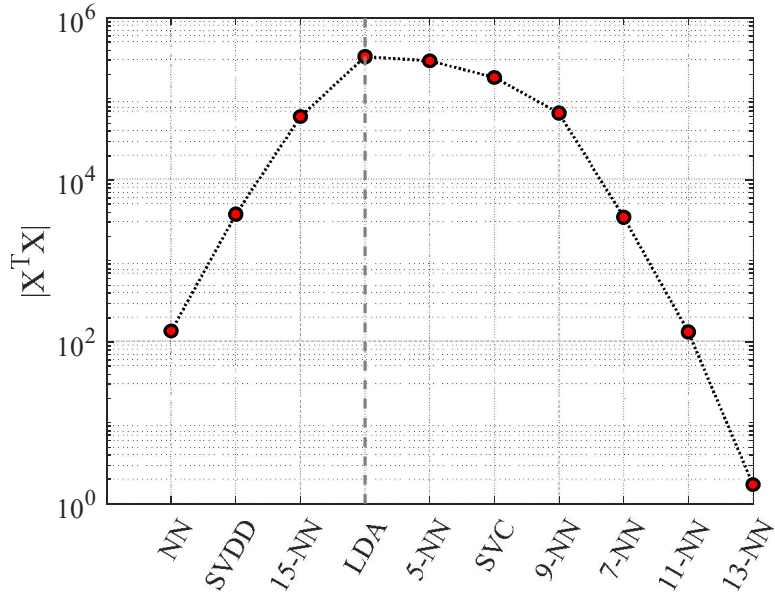


Figure 5. Outcome of the classifier selection procedure by maximizing the determinant of the information matrix constructed by the outputs of the classifiers.

The classifier fusion approaches have been applied to (i) all the trained models, and (ii) the models selected through the selection procedure. The results are presented in Table 7. It indicates that in both cases, the proposed approach leads to the most accurate models but with different weightings. It can also be observed that the proposed classifier selection approach can improve the classification accuracy, regardless of the fusion method. It should be noted that using the proposed combination approach in conjunction with the classifier selection methodology can increase the accuracy from 97.78% (the most accurate model in Table 6) to 100% (the most accurate model in Table 7).

Table 7. Accuracy analysis of the fused model, obtained by using different DST-based approaches. For two scenarios, All: when all the models are used for fusion, and Sel.: when the selected classifiers by the proposed approach are used. In either case, the most accurate models are bold and underlined.

Fusion		M_1	M_2	M_3	M_4	P_0	P_1	P_2	P_3	P_4	P_5	P_6
All	Train	96.32	95.58	96.32	95.58	99.26	99.26	100	100	99.26	99.26	100
	Test	93.33	92.22	93.33	93.33	95.55	95.55	98.89	95.55	97.78	95.55	96.67
Sel.	Train	98.52	99.26	99.26	99.26	100	100	100	99.26	100	99.26	100
	Test	96.67	96.67	94.44	97.78	96.67	95.55	94.44	98.89	100	95.55	96.67

Statistical analysis

In this section, to obtain uncertainty bounds for the accuracy of the classification models, statistical analysis has been done. For this purpose, the whole proposed framework, namely data resampling, classifier training, selection, and fusion, has been carried out 50 times. Their outcomes are presented in Figure 6 in the form of boxplots. In these figures, the mean values are also shown by cross-circle. Figure 6a shows the variation in the accuracy of the single classifiers. It can be seen that the last three methods have higher accuracies than the other methods. Among them, SVC is the most accurate model with the mean of 97.9% for the test dataset.

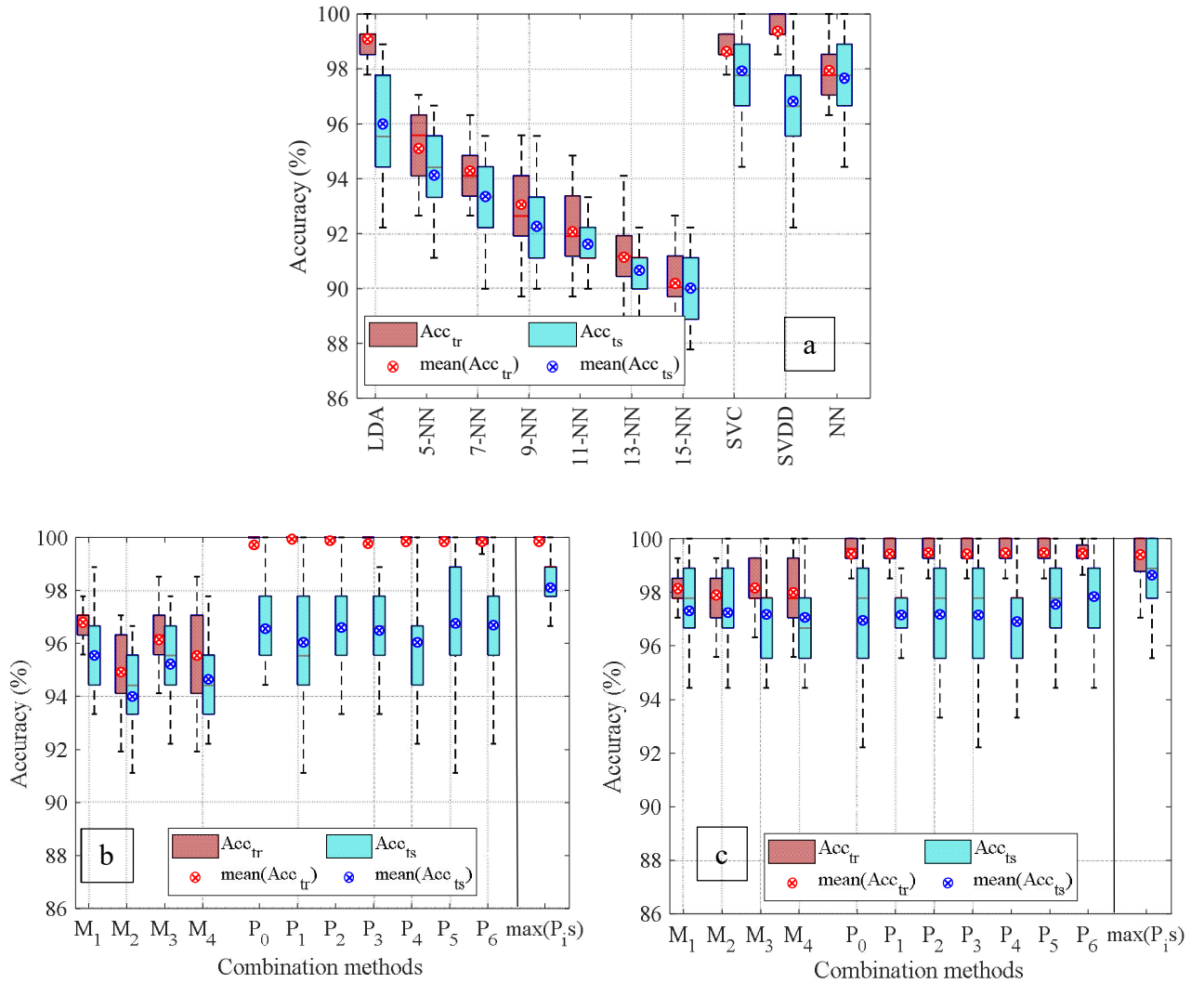


Figure 6. Statistical analysis of the accuracies of (a) single classifiers, (b) fusion of all classifiers, and (c) fusion of selected classifiers. Obtained through 50 repetitions of random data resampling for training samples, classifier training, selection, and combination.

To obtain the variation in the fused model, two scenarios have been investigated:

- (i) all models are used for combination (see Figure 6b)
- (ii) only the models selected by the proposed approach are used for fusion (see Figure 6c).

Each figure contains the classification results for the different fusion methods. It can be seen that the best performance in classification of the blades can be achieved by the proposed classifier selection-fusion technique in the presence of weighting w_5 and the boosting version P_6 .

It should be noted that since the proposed method has been presented with five different weightings and a boosting scheme, at each repetition the maximum accuracy could occur in some of them. To illustrate the benefit of these weightings, at each repetition the maximum accuracy among different versions of the proposed method has been collected and is shown in the last column of Figure 6b and Figure 6c (indicated by $\max(P_i)$). The accuracy increase can be observed. The mean-values of the classification accuracy increased to 98.1% and 98.7% when all models and selected models are respectively used for combination.

The last analysis is about weighting schemes. Figure 7 shows the number of occurrences for each weighting. It indicates that w_6 and w_7 have the best performances in conjunction with the proposed methodology.

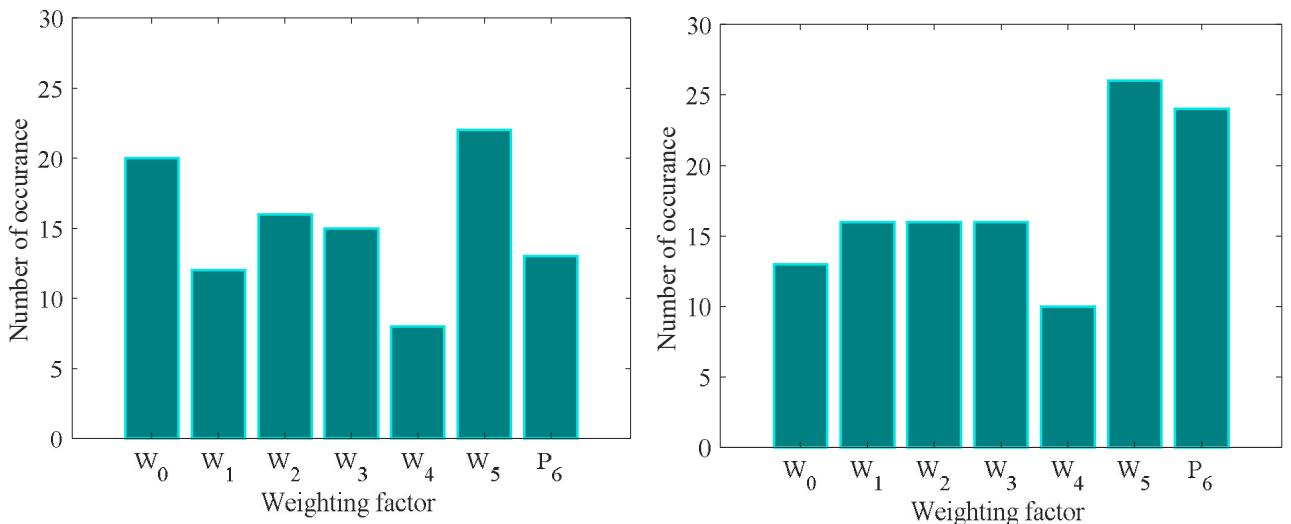


Figure 7. The number of times that different weight factors lead to the fused model with the highest accuracy when all models (left) and selected models (right) were used for combination.

5 Conclusion

In this paper, a multi-classifier selection-fusion framework has been developed to classify geometrically complex parts in terms of their structural quality. The selection algorithm is based on maximizing the information content of the classifiers' output while keeping the diversity in the classifiers set. The Dempster-Shafer theory of evidence was used for classifier fusion. The proposed method has been equipped with five different weightings and one boosting scheme.

To validate the performance of the proposed method, it has been applied to six UCI machine learning datasets. It is also applied to the experimental data measured by the PCRT package. The data was collected from equiax polycrystalline Nickel alloy first-stage turbine blades with complex geometry. The results demonstrated the benefit of employing the proposed selection-fusion framework. By comparing with four DST-based classifier fusion methods, the better performance of the proposed framework in terms of accuracy was observed.

Two new weightings were introduced and together with five other weightings have been investigated. It was shown that, although in general, it is not possible to define a universal weighting that can improve the fusion performance for all applications, the newly introduced weighting and boosting have better impacts on the final classification accuracy than that of the other weightings.

6 Acknowledgment

The authors gratefully acknowledge the ICON project DETECT-ION (HBC.2017.0603) which fits in the SIM research program MacroModelMat (M3) coordinated by Siemens (Siemens Digital Industries Software, Belgium) and funded by SIM (Strategic Initiative Materials in Flanders) and VLAIO (Flemish government agency Flanders Innovation & Entrepreneurship). The authors further acknowledge funding from the Fonds voor Wetenschappelijk Onderzoek FWO (grant 12T5418N). Vibrant Corporation is also gratefully acknowledged for providing anonymous datasets of the blades.

References

- [1] E. Todorov, R. Spencer, S. Gleeson, M. Jamshidinia, and S. M. K. Ewi, "America makes: National additive manufacturing innovation institute (NAMII) project 1: Nondestructive evaluation (NDE) of complex metallic additive manufactured (AM) structures," No. 55028GTH. Edison welding inst inc columbus OH, 2014.
- [2] A. Thompson, I. Maskery, and R. K. Leach, "X-ray computed tomography for additive manufacturing : A review," *Meas. Sci. Technol.*, vol. 27, p. 072001, 2016.

- [3] A. Du Plessis, I. Yadroitsev, I. Yadroitsava, and S. G. Le Roux, “X-Ray microcomputed tomography in additive manufacturing: a review of the current technology and applications,” *3D Print. Addit. Manuf.*, vol. 5, pp. 227–247, 2018.
- [4] E. Pomponi and A. Vinogradov, “A real-time approach to acoustic emission clustering,” *Mech. Syst. Signal Process.*, vol. 40, pp. 791–804, 2013.
- [5] M. Salucci *et al.*, “Real-time NDT-NDE through an innovative adaptive partial least squares SVR inversion approach,” *IEEE Trans. Geosci. Remote Sens.*, vol. 54, pp. 6818–6832, 2016.
- [6] H. J. Lim, H. Sohn, and Y. Kim, “Data-driven fatigue crack quantification and prognosis using nonlinear ultrasonic modulation,” *Mech. Syst. Signal Process.*, vol. 109, pp. 185–195, 2018.
- [7] S. Sambath, P. Nagaraj, and N. Selvakumar, “Automatic defect classification in ultrasonic NDT using artificial intelligence,” *J. Nondestruct. Eval.*, vol. 30, pp. 20–28, 2011.
- [8] F. Guibert, M. Rafrati, D. Rodat, E. Prothon, N. Dominguez, and S. Rolet, “Smart NDT tools: Connection and automation for efficient and reliable NDT operations,” in *19th World Conference on Non-Destructive Testing*, 2016, pp. 1–10.
- [9] T. Schromm, F. Diewald, and C. Grosse, “An attempt to detect anomalies in car body parts using machine learning algorithms,” in *9th Conference on Industrial Computed Tomography*, 2019, pp. 1–5.
- [10] K. Virupakshappa and E. Oruklu, “Investigation of feature inputs for binary classification of ultrasonic NDT signals using SVM and neural networks,” in *62nd International Midwest Symposium on Circuits and Systems (MWSCAS)*, 2019, pp. 638–641.
- [11] M. Abdelniser, A. Abdulbaset, and R. Omar M., “Reducing sweeping frequencies in microwave NDT employing machine learning feature selection,” *Sensors*, vol. 16, pp. 1–14, 2016.
- [12] M. Mishra, A. S. Bhatia, and D. Maity, “Support vector machine for determining the compressive strength of brick - mortar masonry using NDT data fusion (case study :Kharagpur, India),” *SN Appl. Sci.*, vol. 1, pp. 1–11, 2019.
- [13] A. Mayes *et al.*, “Process compensated resonance testing (PCRT) inversion for material characterization and digital twin calibration,” *AIP Conf. Proc.*, vol. 2102, p. 020019, 2019.
- [14] R. H. Nath, C. C. Grupke, C. Leonard, and M. K. Johnson, “Classical nondestructive testing techniques do not correlate with strength as does process compensated resonant testing,” in *Shape Casting: 4th International Symposium 2011*, 2011, pp. 233–240.
- [15] L. Jauriqui and L. Hunter, “A more comprehensive NDE: PCRT for ceramic components,” in *AIP Conference Proceedings*, 2011, vol. 1335, p. 997.
- [16] J. V. Heffernan *et al.*, “Process compensated resonance testing models for quantification of creep damage in single crystal nickel-based superalloys,” *Mater. Eval.*, vol. 75, pp. 941–952, 2017.
- [17] R. Livings, A. Mayes, E. Biedermann, J. Heffernan, L. Jauriqui, and S. Mazdiyasni, “Detection of microtexture regions in titanium turbine engine disks using process compensated resonance testing: A modeling study,” in *AIP Conference Proceedings*, 2019, vol. 2102, p. 020022.
- [18] L. Cheng, V. Yaghoubi, W. Van Paepegem, and M. Kersemans, “Mahalanobis classification system (MCS) integrated with binary particle swarm optimization for robust quality classification of complex metallic turbine blades,” *Mech. Syst. Signal Process.*, vol. 146, p.

107060, Jan. 2021.

- [19] T. Hastie, R. Tibshirani, and J. Friedman, *The Elements of Statistical Learning: Data Mining, Inference, and Prediction*. Springer Science & Business Media, 2009.
- [20] S. Rothe, B. Kudszus, and D. Söfftker, “Does classifier fusion improve the overall performance? Numerical analysis of data and fusion method characteristics influencing classifier fusion performance,” *Entropy*, vol. 21, p. 866, 2019.
- [21] M. P. Ponti, “Combining Classifiers: from the creation of ensembles to the decision fusion,” in *24th SIBGRAPI Conference on Graphics, Patterns, and Images Tutorials*, 2011, pp. 1–10.
- [22] Y. Pan, L. Zhang, X. Wu, and M. J. Skibniewski, “Multi-classifier information fusion in risk analysis,” *Inf. Fusion*, vol. 60, pp. 121–136, Aug. 2020.
- [23] Q. He *et al.*, “Feasibility study of a multi-criteria decision-making based hierarchical model for multi-modality feature and multi-classifier fusion: Applications in medical prognosis prediction,” *Inf. Fusion*, vol. 55, pp. 207–219, Mar. 2020.
- [24] B. Quost, M. H. Masson, and T. Denœux, “Classifier fusion in the Dempster-Shafer framework using optimized t-norm based combination rules,” *Int. J. Approx. Reason.*, vol. 52, pp. 353–374, 2011.
- [25] D. Ruta and B. Gabrys, “Classifier selection for majority voting,” *Inf. fusion*, vol. 6, pp. 63–81, 2005.
- [26] Y. S. HUANG, K. LIU, and C. Y. SUEN, “The combination of multiple classifiers by a neural network approach,” *Int. J. Pattern Recognit. Artif. Intell.*, vol. 09, pp. 579–597, 1995.
- [27] L. I. Kuncheva, J. C. Bezdek, and R. P. W. Duin, “Decision templates for multiple classifier fusion: An experimental comparison,” *Pattern Recognit.*, vol. 34, pp. 299–314, 2001.
- [28] N. Pizzi and W. Pedrycz, “Aggregating multiple classification results using fuzzy integration and stochastic feature selection,” *Int. J. Approx. Reason.*, vol. 51, pp. 883–894, 2010.
- [29] G. Rogova, “Combining the results of several neural network classifiers,” *Stud. Fuzziness Soft Comput.*, vol. 219, pp. 683–692, 2008.
- [30] A. Al-Ani and M. Deriche, “A new technique for combining multiple classifiers using the Dempster-Shafer theory of evidence,” *J. Artif. Intell. Res.*, vol. 17, pp. 333–361, 2002.
- [31] X. Deng, Q. Liu, Y. Deng, and S. Mahadevan, “An improved method to construct basic probability assignment based on the confusion matrix for classification problem,” *Inf. Sci. (Ny)*, vol. 340–341, pp. 250–261, May 2016.
- [32] J. Qian, · Xingfeng Guo, · Yong Deng, and Y. Deng, “A novel method for combining conflicting evidences based on information entropy,” vol. 46, pp. 876–888, 2017.
- [33] F. Xiao, “A novel evidence theory and fuzzy preference approach-based multi-sensor data fusion technique for fault diagnosis,” *Sensors (Switzerland)*, vol. 17, no. 11, Nov. 2017.
- [34] F. Xiao and B. Qin, “A weighted combination method for conflicting evidence in multi-sensor data fusion,” *Sensors (Switzerland)*, vol. 18, no. 5, May 2018.
- [35] L. Fei, J. Xia, Y. Feng, and L. Liu, “A novel method to determine basic probability assignment in Dempster–Shafer theory and its application in multi-sensor information fusion,” *Int. J. Distrib. Sens. Networks*, vol. 15, no. 7, p. 155014771986587, Jul. 2019.

- [36] Z. Wang, J. Gao, R. Wang, Z. Gao, and Y. Liang, “Fault recognition using an ensemble classifier based on Dempster–Shafer Theory,” *Pattern Recognit.*, vol. 99, p. 107079, Mar. 2020.
- [37] D. Dua and C. Graff, “UCI machine learning repository,” 2017.
- [38] G. Shafer, “Dempster’s rule of combination,” *Int. J. Approx. Reason.*, vol. 79, pp. 26–40, 2016.
- [39] T. Denœux, “Logistic regression, neural networks and Dempster–Shafer theory: A new perspective,” *Knowledge-Based Syst.*, vol. 176, pp. 54–67, 2019.
- [40] L. Xu, A. Krzyżak, and C. Y. Suen, “Methods of Combining Multiple Classifiers and Their Applications to Handwriting Recognition,” *IEEE Trans. Syst. Man Cybern.*, vol. 22, no. 3, pp. 418–435, 1992.
- [41] C. R. Parikh, M. J. Pont, and N. Barrie Jones, “Application of Dempster-Shafer theory in condition monitoring applications: A case study,” *Pattern Recognit. Lett.*, vol. 22, no. 6–7, pp. 777–785, May 2001.
- [42] F. Xiao, “Multi-sensor data fusion based on the belief divergence measure of evidences and the belief entropy,” *Inf. Fusion*, vol. 46, pp. 23–32, Mar. 2019.